Superexponential fluctuation relation for dichotomous work reservoir systems

Sílvio M. Duarte Queirós
Centro Brasileiro de Pesquisas Físicas and National Institute of Science and Technology for Complex Systems, 150 Rua Dr. Xavier Sigaud, 22290-180 Rio de Janeiro, Rio de Janeiro, Brazil
(Received 25 April 2016; published 17 October 2016)

This paper introduces an analytical description of the probability density function of the dissipated and injected powers $p(j_{\rm dis})$ and $p(j_{\rm inj})$, respectively, in a paradigmatic nonequilibrium damped system in contact with a work reservoir that is analytically represented by telegraph noise and to which one can assign an effective temperature. This approach is able to overcome the well-known impossibility of obtaining closed solutions to steady-state distributions of this system and allows determining a superexponential fluctuation relation of the injected power, which is not even asymptotically exponential as for (shot-noise) Poissonian reservoirs. In the white-noise limit, that relation converges to the exponential formula that is standard in thermal systems; however, the distribution of the injected power remains quite different from that of the latter instance. Surprisingly, it is actually shown that a Gaussian distribution, which is archetypal of thermal systems, for the injected power can be achievable only for athermal reservoirs of this kind.

DOI: 10.1103/PhysRevE.94.042114

I. INTRODUCTION

It is now more than well established that several nonequilibrium systems are best described by generalized Langevin equations where the stochastic component of the force is statistically described by a distribution other than the Gaussian one [1–9]. Such revamping of the Langevin equation can stem from many different factors; the following are among the most typical we can mention: (a) The collisions between the system and the particles of the embedding medium (the reservoir) occur at such low rates that the central-limit theorem, which leads to the Gaussian distribution of the noise, is a poor approximation as it happens with granular gases [10], the Andersen thermostat [11], and colloidal systems [12]; (b) the system is subject to random pulses of injected power similarly to molecular motors running on ATPase [7,13–15]; and (c) dynamically, the system evolves resembling a random tug of war as it does in nanomechanical problems such as intracellular bidirectional transport on cytoskeletal filaments mediated by two sets of molecular motors, namely, the kinesin-1 and cytoplasmic dynein [16], the dynamics of calcium ions in blood plasma [17], and some types of ratchets [18].

In situations (a) and (b), the stochastic term usually corresponds to a (Poisson) shot noise [10,19,20], whereas problems of type (c) are best related to telegraph noise ζ, also known as dichotomous or two-state Brownian noise [1,21], i.e., a stochastic process where the variable randomly alternates between two values at given average rates and whose treatment in the probability space must be performed by means of the respective master equation. Aside from the situations I have cited, the telegraph noise also provides a quantitative description of transport properties in amorphous materials [22], chromatography [23], quantum effects [24], and fluctuations of photovoltaics in power grids [25], among other problems.

Due to its analytical complexity, systems involving dichotomous noise are often treated by considering overdamping regimes and assuming equal transition rates between symmetrical states of the noise as well [26–28]. Despite these simplifications, the achievement of fully analytical and closed solutions to the probabilistic descriptions of the position x and the velocity v is quite limited. Moreover, such solutions are impossible in the damped regime. If calculations are already that restricted for those chief observables, the achievement of closed distributions of thermostatistical quantities, such as the power, is far fetched. Hereinafter, I will show that the blending of the statistical knowledge (derived from the dynamics of the system) with adequate distribution functions paves the way to the probabilistic description of the power. The fact that the properties of the system include a robust nonexponential, actually superexponential, fluctuation relation (FR) for the injected power $j_{\rm inj}$ disagrees with its usual form [2,3]

$$p(|\mathcal{O}|)/p(-|\mathcal{O}|) = \exp[2\mu|\mathcal{O}|/\sigma^2], \tag{1}$$

where μ and σ^2 are the average and the variance of the physical quantity $\mathcal{O}$, respectively.

The rest of this paper is organized as follows. In Sec. II the dynamical equations ruling the evolution of our system are introduced as well as the features of the dichotomous work reservoir. In Sec. III, the results of the probabilistic descriptions of the dissipated and the injected power are presented. Section IV summarizes and discusses the results obtained and their impact on future research.

II. PROBLEM FORMULATION

Herein, as in a plethora of other relevant studies [3], I assume the quintessential damped nonequilibrium system, with mass m, whose position x [with velocity $v \equiv \frac{dx(t)}{dt}$] is ruled by

$$m\frac{d^2x(t)}{dt^2} = -\gamma\frac{dx(t)}{dt} - kx(t) - \zeta_t. \tag{2}$$

The parameter γ relates to the friction the system is subject to and ζ is the stochastic force describing the interaction between the particle and the dichotomous reservoir, as already mentioned and to be fully characterized shortly. The damping is established by the harmonic potential $k\,x^2/2$, mimicking either physical traits of the system or simply the action of an optical tweezers (the behavior of which is known to be very close to harmonicity [29]) that is used in order to not let it diffuse.

For the sake of simplicity, I consider wonted features for the telegraph noise:[1] It assumes two symmetric values $\zeta_t = \{-a,a\}$, swinging from one to the other with the same transition rate μ. In the stationary state [as well as at every instant t], the process $\{\zeta_t\}$ always follows a bimodal distribution

$$f(\zeta) = \tfrac{1}{2}\delta(\zeta + a) + \tfrac{1}{2}\delta(\zeta - a) \tag{3}$$

and has a colored correlation function with frequency $\alpha = 2\mu$,

$$\langle \zeta(t_1)\zeta(t_2)\rangle = a^2 e^{-\alpha|t_1 - t_2|} \tag{4}$$

[further moments $\langle \zeta(t_1), \ldots, \zeta(t_n)\rangle$ are discussed in Appendix A]. Taking into account the two-state properties of the noise, the reservoir is an athermal work reservoir since it performs work on the massive system by either pulling or pushing it during random periods of time.

Equations (3) and (4) establish that ζ cannot be treated within the Lévy-Itô theorem on the decomposition of the measure [30]. Moreover, such features impose two important properties on Eq. (2): (i) Since ζ is colored and the dissipation term $-\gamma \frac{dx(t)}{dt}$ has no kernel, the fluctuation-dissipation relation is not verified and thus the dichotomous work reservoir is of the external class [1,31]; (ii) allowing for its bimodality, the particle cannot explore its full phase space,[2] which implies that the system is effectively nonlinear.

Several thermostatistical aspects of Eq. (2) were recently studied in [32], where it was shown that in the steady state x is sub-Gaussian[3] as well as v for most of α. Furthermore, it is possible to define an energy scale ($k_B = 1$) therein called the Marconi temperature

$$\mathcal{T} \equiv \frac{\hat{\gamma} - \gamma}{\gamma \hat{k}} a^2 = m\langle v^2\rangle \tag{5}$$

[$\hat{\gamma} \equiv \gamma + m\alpha$ and $\hat{k} \equiv k + \alpha(\gamma + m\alpha)$], which allows writing the entropy production (exchange) rate in the steady state Π (Ψ) in the exact same form as of a typical thermal system [33]

$$\Pi = -\Psi = \frac{\gamma}{m}. \tag{6}$$

Each of two entropy contributions is related to the power injected by the work reservoir and the power dissipated by the system, respectively,

$$j_{\rm inj}(t) \equiv \zeta_t v(t), \quad j_{\rm dis}(t) \equiv -\gamma v(t)^2, \tag{7}$$

which control the variation of energy in the system. The large deviation behavior of both powers, i.e., the work and heat fluxes

$$J_{(\cdot)}(\Xi) \equiv \int_0^{\Xi} j_{(\cdot)}(t)dt, \tag{8}$$

was analyzed in [32], showing that its distribution, i.e., the large deviation function (LDF), is single sided and functionally the same in both cases. That is not surprising taking into account the system attains a steady state. It was also understood that the power or work LDF converges relatively fast to the large deviation function obtained when the mechanical system is in contact with a thermal reservoir at a temperature T that is (numerically) equal to the fixed Marconi temperature and subject to the same dissipation constant γ.

In spite of the fact that the large deviation function of $J_{(\cdot)}(\Xi)$ allows understanding the likelihood of the system experiencing a weighty long-term departure of the power from its expected value $\langle J_{\rm inj}(\Xi)\rangle = |\langle J_{\rm dis}(\Xi)\rangle| \propto \frac{\gamma}{m}\mathcal{T}\Xi$, it is also important to quantify the probability of a sudden overpowering or a significant power depletion to the system; this cannot be computed from $J_{(\rm inj)}$, but by analyzing the probabilities of $j_{\rm inj}$ instead. In other words, while $j_{\rm dis} \leqslant 0$ by default, $j_{\rm inj}$ is undefined, which makes it relevant to learn to what extent a dichotomous work reservoir injects energy in the system in opposition to the effect of taking it out, an assessment we can make explicit from the FR $p(|j_{\rm inj}|)/p(-|j_{\rm inj}|)$.

In what follows, I shall be mainly interested in assessing the impact of the color of the noise on the probability density function of the powers. Therefore, $\mathcal{T}$ is set as

$$\langle v^2\rangle = \frac{\mathcal{T}}{m} = \text{const}\,\forall_\alpha, \tag{9}$$

so that in modifying α, the intensity of the noise must change as $a \sim \mathcal{T}^{1/2}\alpha^{1/2}$. In the white-noise (WN) limit $\alpha \to \infty$, the value of a goes to infinity, yet $f(\zeta)$ preserves its bimodality at all α.

III. RESULTS

A. Distribution of the dissipated power

Let me first briefly describe the steady-state distribution $p(j_{\rm dis})$ in its prevalent and more relevant regime of sub-Gaussianity (platykurticness) with further analytical details provided in Appendix D. For the regime $\mu \to 0$, the results are presented in Appendix C.

Bearing in mind Eq. (7), the distribution $p(j_{\rm dis})$ is easily obtained from the velocity distribution $p(v)$, using the law of the conservation of the probability

$$p(j_{\rm dis})dj_{\rm dis} = p(v)dv. \tag{10}$$

The distribution $p(v)$ does not have a closed form in the damped regime and it was previously shown that it can have (lepto)platykurtic behavior for α (<)> α^* [32].

Heeding that the platykurticness hints at compact support distributions and recalling that numerical simulations showed that, in a log-lin scale, $p(v)$ is prone to flatness at its center [32], it can be asserted that the distribution is well described by

$$p(v) = \frac{1}{\mathcal{Z}}\left[1 - \frac{\mathcal{B}}{\nu}|v|^{\delta}\right]^{\nu}. \tag{11}$$

The values of the parameters $\mathcal{B}$, ν, and δ are to be obtained by the matching of the second-, fourth-, and sixth-order statistical moments given by Eq. (2) and those of the ansatz (D9). The statistical moments of the former are obtained by employing a method based on the Fourier-Laplace transform explained in

[1] We use $\langle\cdots\rangle$ to represent averages over samples and $\langle\langle\cdots\rangle\rangle$ for the cumulants.

[2] Except in the limit $\alpha \to \infty$.

[3] Such behavior is typical of variables with compact support, which in this case leads to the effective nonlinearity of the potential.

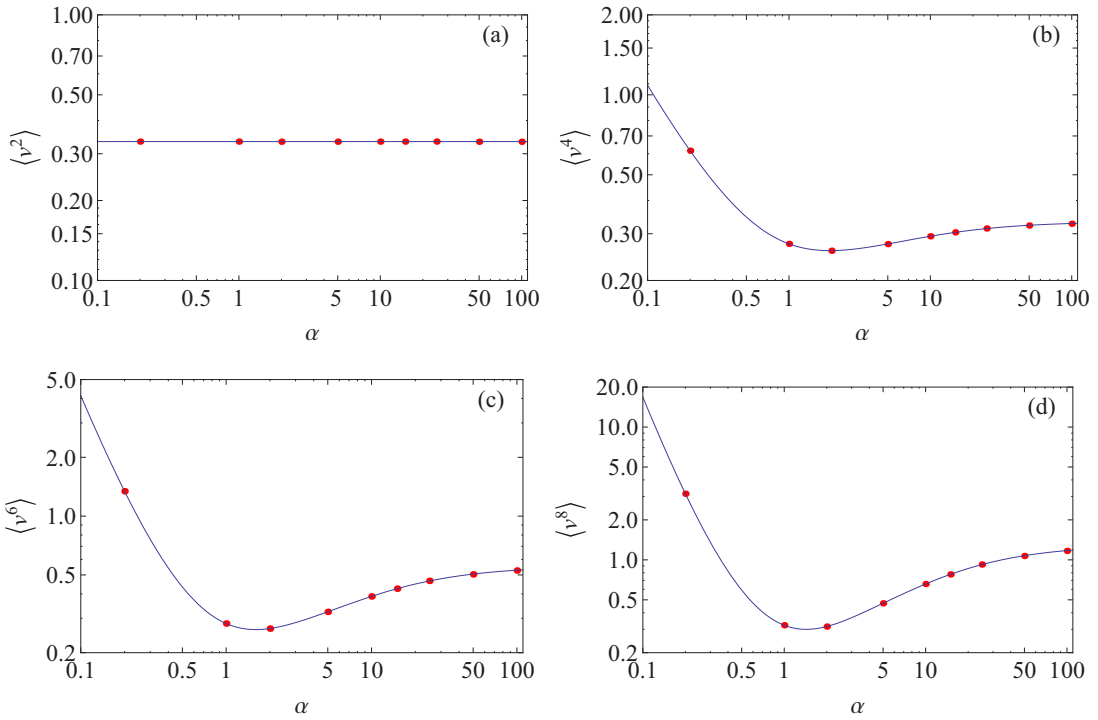

FIG. 1. Second-, fourth-, sixth-, and eighth-order moment of the velocity v color of the noise α in log-log scale assuming $k = m = \gamma = 1$ and $\mathcal{T} = 1/3$. The solid lines are obtained analytically from Eq. (2) and the dots are the values from the numerical implementation of Eq. (2).

Appendix A, whereas for the latter the even moments read[4]

$$\langle v^{2n} \rangle_p = \left(\frac{\nu}{\mathcal{B}}\right)^{2n/\delta} \frac{\Gamma\left[\frac{2n+1}{\delta}\right]\Gamma\left[1+\frac{1}{\delta}+\nu\right]}{\Gamma\left[\frac{1}{\delta}\right]\Gamma\left[1+\frac{2n+1}{\delta}+\nu\right]}, \quad n \in \mathbb{N}. \tag{12}$$

Nevertheless, in Fig. 1, we show a comparison between the analytical expressions for the moments obtained from the dynamics and the numerical implementation of the model. Since our problem is described by five independent parameters (m, γ, k, α, and $\mathcal{T}$), an approach involving up to five equations is totally meaningful.

Shown in Fig. 2 is the convergence of ν and δ to their white-noise limits, which are equal to zero and two, respectively, as expected for a Gaussian distribution. Specifically, the following asymptotic behavior can be verified:

$$\nu \sim \alpha, \quad \delta - 2 \sim \alpha^{-2},$$

stressing the fact that $p(v)$ asymptotically tends to a exponential functional with α going to infinity. The error

$$\epsilon_8(v) \equiv 100 \left| \frac{\langle v^8 \rangle_p - \langle v^8 \rangle}{\langle v^8 \rangle} \right| \tag{13}$$

of this ansatz is never larger than 0.2% in $\langle v^8 \rangle$ (see Fig. 3), whereas the error for $\delta = 2$ (taken as standard) is always at least ten times as large as the ansatz (D9). In both cases, it goes asymptotically as $\epsilon_8(v) \sim \alpha^{-2}$.

For $\alpha = 3.20\ldots$, which corresponds to three changes in the value of ζ within the scale of relaxation (in average), the value obtained is $\delta = 2$ (and ν finite), with a kurtosis close to the triangle distribution, and for $\alpha = 2.15\ldots$ one has $\nu = 1$ ($\delta \neq 2$). For $\alpha = 6.028\ldots$, the two values of $\langle v^8 \rangle$ concur and hence the two distributions coincide up to eighth order.

Plotted in Fig. 4 is a comparison between the empirical distribution function obtained by numerical implementation of Eqs. (2) and (D9) for $\delta \neq 2$ and $\delta = 2$. Since the kurtosis of the velocity is reminiscent of a distribution with compact support distribution, the panels in that figure show that the major impact of $\delta \neq 2$ lies in the determination of the upper and lower bounds of the distribution. As a result, the steady-state distribution of the dissipated power reads

$$p(|j_{\rm dis}|) = \frac{1}{\mathcal{Z}} \sqrt{\frac{\gamma}{|j_{\rm dis}|}} \left[1 - \frac{\mathcal{B}}{\nu} \left| \frac{j_{\rm dis}}{\gamma} \right|^{\delta/2} \right]^{\nu}. \tag{14}$$

B. Distribution of the injected power and its fluctuation relation

To determine $p(j_{\rm inj})$, whence one gets the fluctuation relation, I start by looking at the limit $\alpha \to \infty$ for which $p(v)$ is a Gaussian distribution. In addition, the velocity and the telegraph force are correlated for all α, with that correlation

[4]The full expressions are presented in Appendix D for the sake of conciseness.

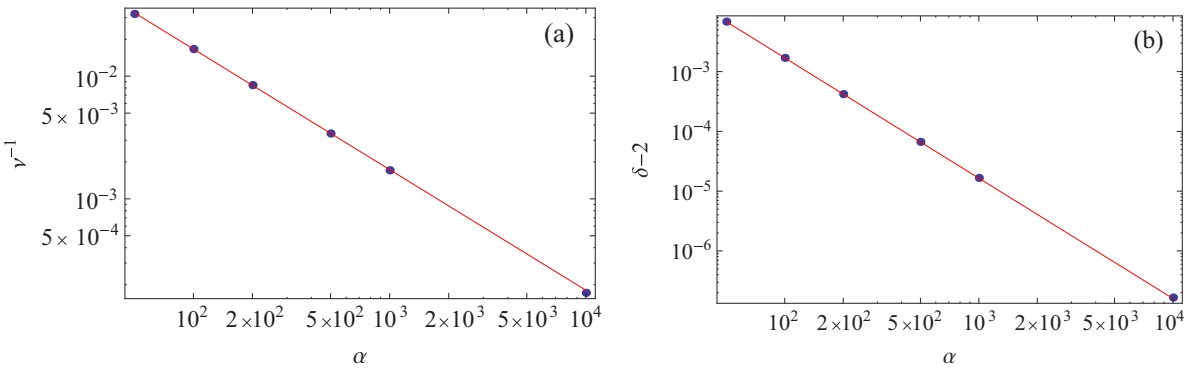

FIG. 2. Asymptotic behavior of (a) ν and (b) δ vs α for the case $k = m = \gamma = 1$ and $\mathcal{T} = 1/3$. The slope of each line is equal to (a) -1 and (b) -2.

being precisely the average injected power[5]

$$\overline{v(t)\zeta(t)} = \overline{j_{\rm inj}} = \frac{\gamma\mathcal{T}}{m}. \tag{15}$$

This permits one to surmise that at each instant the velocity is written as the superposition of two independent contributions

$$v(t) = c\zeta(t) + \xi(t), \tag{16}$$

where the first term on the right-hand side yields Eq. (15) and the second, $\xi(t)$, is a stochastic variable, with velocity units, that is Gaussian distributed with variance σ_ξ^2 so that

$$c^2\sigma_\zeta^2 + \sigma_\xi^2 = \frac{\mathcal{T}}{m}. \tag{17}$$

Moreover, Eq. (16) tacitly implies that

$$\langle\zeta(t)\xi(t')\rangle = 0\,\forall_{t,t'}, \tag{18}$$

that is to say,

$$c = \frac{\mathcal{T}}{m}\frac{\gamma}{a^2}, \quad \sigma_\xi^2 = \frac{\mathcal{T}}{m}\left[1 - \frac{\mathcal{T}}{m}\left(\frac{\gamma}{a}\right)^2\right]. \tag{19}$$

In the end, from Eqs. (15)–(19),[6]

$$p_{\rm WN}(j_{\rm inj}) = \iint_{-\infty}^{+\infty} \frac{1}{\sqrt{2\pi\sigma_\xi^2}} \exp\left[-\frac{\xi^2}{2\sigma_\xi^2}\right] f(\zeta) \times \delta(j_{\rm inj} - \zeta[c\zeta + \xi])d\xi d\zeta, \tag{20}$$

which yields

$$p_{\rm WN}(j_{\rm inj}) = \frac{1}{\sqrt{2\pi}a\sigma_\xi}\exp\left[-\frac{(j_{\rm inj} - ca^2)^2}{2(a\sigma_\xi)^2}\right] = \frac{1}{\sqrt{2\pi}\sigma_{j_{\rm inj}}}\exp\left[-\frac{(j_{\rm inj} - \langle j_{\rm inj}\rangle)^2}{2\sigma_{j_{\rm inj}}^2}\right], \tag{21}$$

i.e., a Gaussian distribution centered at

$$ca^2 = \frac{\gamma\mathcal{T}}{m} = \langle j_{\rm inj}\rangle. \tag{22}$$

Contrarily to $j_{\rm dis}$, the injected power assumes both positive and negative values, which renders the fluctuation relation

$$\frac{p_{\rm WN}(|j_{\rm inj}|)}{p_{\rm WN}(-|j_{\rm inj}|)} = \exp\left[\frac{2c}{\sigma_\xi^2}|j_{\rm inj}|\right]. \tag{23}$$

The significance of Eqs. (21) and (23) is made by comparing them with thermal reservoir results [33]; in that case[7]

$$p(j_{\rm inj}) \propto \exp[\mathsf{J}_1 j_{\rm inj}]K_0[-\mathsf{J}_2|j_{\rm inj}|], \tag{24}$$

which is neatly non-Gaussian and different from the dichotomous work reservoir (21). This is a flummoxing result; explicitly, while a thermal reservoir does not yield a Gaussian distribution for $p(j_{\rm inj})$, even in the linear case, it is not expected at all that such a connotative distribution would emerge within an athermal reservoir scenario.

Complementarily, recalling the results for the athermal Poissonian reservoir [20], the singular counterpart of thermal reservoirs, one grasps that the ubiquity of Eq. (23) goes beyond the discussion framed within the Lévy-Itô theorem as ζ is colored and always bimodal. As a consequence, the canonical fluctuation relation (1) is above all linked to the infinite rate at which the value the system-reservoir interaction changes.

Having the white-noise limit in hand, one moves on to obtain $p(j_{\rm inj})$ for finite values of α. From analytical calculations of the kurtosis $\gamma_2(j_{\rm inj})$ (see the dot-dashed line in Fig. 5) it is possible to perceive that $p(j_{\rm inj})$ is also typically platykurtic and converges to the Gaussian distribution.

In furtherance of succinctness, I address in Appendix D the formulas of the moments of the injected power and present in Fig. 6 comparisons between the analytical calculations of the moments of the injected power (up to fifth order) and the results from numerical implementations of the model. Taking into account these features, one could be tempted to assert for the distribution of the injected power a compact support function similar to $p(v)$. However, it is crucial to heed that the

[5] $\overline{\mathcal{O}^n}$ stands for time averaging. In the steady state it concurs with sample averaging $\langle\mathcal{O}^n\rangle$.

[6] Since we work with a fixed Marconi temperature, the value of the amplitude a increases as we approach the noise limit. Therefore, $\lim_{\alpha\to\infty} c\zeta = 0^{\pm}$.

[7] For the explicit form see Eq. (35) and Fig. 6 in [33].

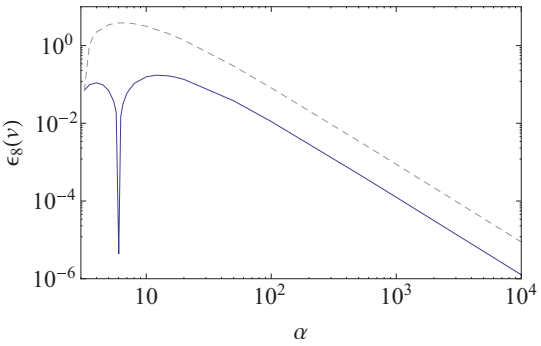

FIG. 3. The solid line represents the error $\epsilon_8(v)$ vs α for the proposal (D9). The dashed gray line is obtained by considering $\delta = 2$ for comparison ($k = m = \gamma = 1$ and $\mathcal{T} = 1/3$).

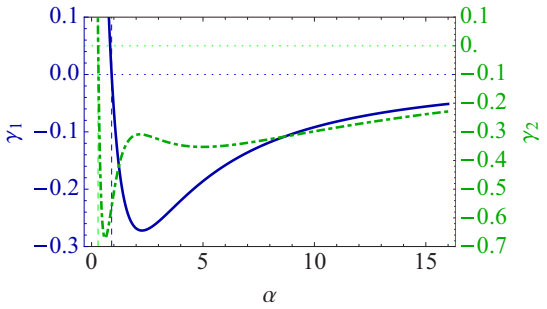

FIG. 5. Skewness γ_1 (solid blue line, left ordinate axis) and kurtosis γ_2 (dot-dashed green line, right ordinate axis) of the injected power vs α with $m = k = \gamma = 1$ and $\mathcal{T} = 1/3$. The vertical lines represent the values of α at which both curves cross the origin, $\alpha = 0.900\ldots$ and $\alpha = 0.295\ldots$, respectively.

skewness $\gamma_1(j_{\rm inj})$ vanishes only in the white-noise limit (see full line in Fig. 5). To accommodate $\gamma_1(j_{\rm inj})$ and $\gamma_2(j_{\rm inj})$ one asserts

$$p(j_{\rm inj}) = \left[1 - \frac{\mathcal{B}}{\nu}(j_{\rm inj} - \omega)^2\right]^{\nu} \left\{\mathcal{A} + \varphi(j_{\rm inj} - \omega)\mathcal{A}' \times {}_2F_1\left[\frac{1}{2}, \nu; \frac{3}{2}; -\frac{\mathcal{B}\varphi^2}{\nu}(j_{\rm inj} - \omega)^2\right]\right\} \tag{25}$$

(φ is the skew parameter), which in the limit $\nu \to \infty$ converges to the skewed Gaussian distribution. This approach is particularly valid as the skewness of $p(j_{\rm inj})$ is not extreme. In determining the values of the parameters of $p(j_{\rm inj})$ it was found that the error

$$\epsilon_5(j_{\rm inj}) \equiv 100\left|\frac{\langle j_{\rm inj}^5\rangle_p - \langle j_{\rm inj}^5\rangle}{\langle j_{\rm inj}^5\rangle}\right|. \tag{26}$$

is never larger than 1.7% in $\langle j_{\rm inj}^5\rangle$, as plotted in Fig. 7.

The average value $\langle j_{\rm inj}\rangle = \frac{\gamma}{m}\mathcal{T}$ differs from ω, but the latter converges to the former as $\alpha \to \infty$. It must be noted that this convergence is slow because φ goes to zero as $\alpha^{-1/2}$ (see Fig. 8). The calculations show that the cumulants of order larger than the second vanish (see Fig. 5), confirming the Gaussian distribution (21).

With Eq. (25) in hand, one is in the position to discuss the FR for this class of reservoir, to which one compares the present and previous results for the thermal and other athermal situations. For Poissonian reservoirs, a deviation from the usual exponential behavior was verified as well [20]; however, the perturbation to the thermal FR is composed of terms whose coefficients depend on the modified Bessel function and it tends to the standard exponential form for large values of $|j_{\rm inj}| \in \mathbb{R}_0^+$. On the contrary, for $\alpha \neq 0$ dichotomous reservoirs, one observes the emergence of superexponential growth of the FR. Moreover, the power-law decay of the hypergeometric function (as large values of $j_{\rm inj}$ become available) establishes another striking difference from the Poissonian case. Close to its limit $\hat{j}_{\rm inj} \equiv \sqrt{\nu/\mathcal{B}} - \omega = -j_{\rm inj}^{(\rm min)}$, the fluctuation relation can be written as

$$\frac{p(|j_{\rm inj}|)}{p(-|j_{\rm inj}|)} \approx \left(\frac{\nu - \mathcal{B}(|j_{\rm inj}| - \omega)^2}{\nu - \mathcal{B}(|j_{\rm inj}| + \omega)^2}\right)^{\nu} \frac{1 + \varphi A_1(|j_{\rm inj}| - \omega)}{1 - \varphi B_1(|j_{\rm inj}| + \omega)}, \tag{27}$$

where $j_{\rm inj} \lesssim \hat{j}_{\rm inj}$ and $\varphi = \varphi(\alpha) < 1$. As α grows, we have $\nu, \hat{j}_{\rm inj} \to \infty$ and $\varphi \to 0$; the contribution to the skewness zeros out and Eq. (27) concurs with Eq. (23).

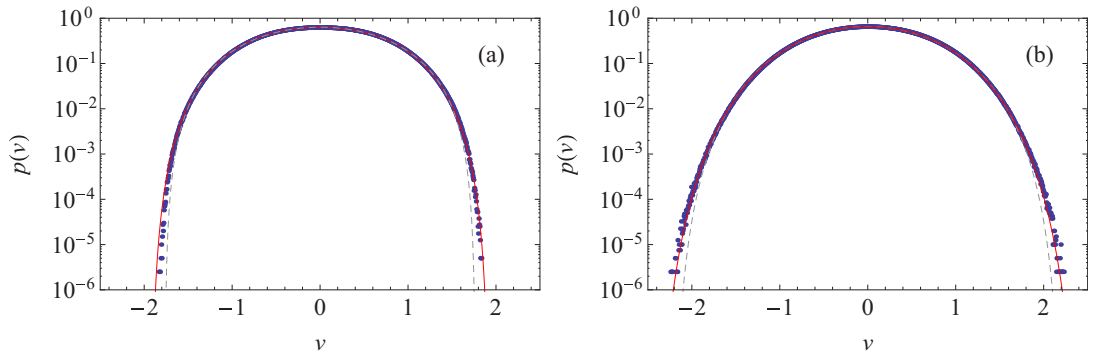

FIG. 4. Dots represent the empirical distribution function obtained from the dynamics (2) with (a) $\alpha = 5$ and (b) $\alpha = 10$ with $m = k = \gamma = 1$ and $\mathcal{T} = 1/3$. The solid red lines correspond to Eq. (D9) with $\delta \neq 2$ and the dashed gray lines set $\delta = 2$. For the former case (a) $\mathcal{B} = 1.018\ldots$, $\nu = 4.645\ldots$, and $\delta = 2.241\ldots$ and (b) $\mathcal{B} = 1.053\ldots$, $\nu = 8.404\ldots$, and $\nu = 2.136\ldots$ and for the latter (a) $\mathcal{B} = 1.004\ldots$ and $\nu = 3.165\ldots$ and (b) $\mathcal{B} = 1.045\ldots$ and $\nu = 5.860\ldots$.

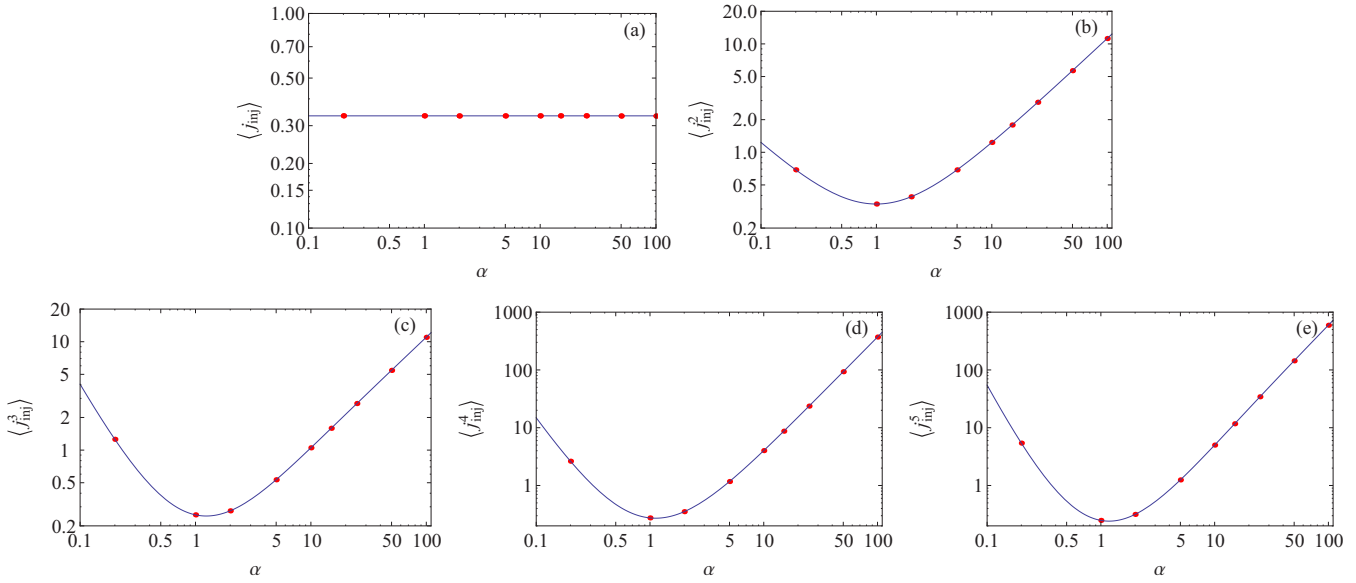

FIG. 6. Solid lines represent in a log-log scale the moments analytically obtained from the dynamics and the dots are the values obtained from the numerical implementation of Eq. (2) vs α ($k = m = \gamma = 1$ and $\mathcal{T} = 1/3$).

Alternatively, for small values of $j_{\rm inj}$, Eq. (25) tends to

$$\frac{p(|j_{\rm inj}|)}{p(-|j_{\rm inj}|)} \approx \left(1 - 4\frac{\omega\mathcal{B}}{\omega^2\mathcal{B} - \nu}|j_{\rm inj}|\right)^{\nu} \times \left(1 + \mathcal{C}\,{}_2F_1\left[\frac{1}{2}, \nu; \frac{3}{2}; -\frac{\mathcal{B}\omega^2\alpha^2}{\nu}\right]|j_{\rm inj}| + \ldots\right), \tag{28}$$

which implies that close to zero the fluctuation relation increases with slope equal to

$$\mathcal{C} = 4\varphi\sqrt{\frac{\mathcal{B}}{\pi\nu}}\frac{\Gamma[\nu]}{\Gamma\left[\nu - \frac{1}{2}\right]}\,{}_2F_1\left[\frac{1}{2}, \nu; \frac{3}{2}; -\frac{\mathcal{B}\omega^2\alpha^2}{\nu}\right]. \tag{29}$$

Shown in Fig. 9 is shown a comparison between the numerical simulation results and the fluctuation relation obtained from Eq. (25), which recovers the standard relation matching with Eq. (23) as well with

$$\exp[4\omega\mathcal{B}|j_{\rm inj}|] = \exp\left[2\langle j_{\rm inj}\rangle|j_{\rm inj}|/\sigma^2_{j_{\rm inj}}\right] \tag{30}$$

in the white-noise limit.

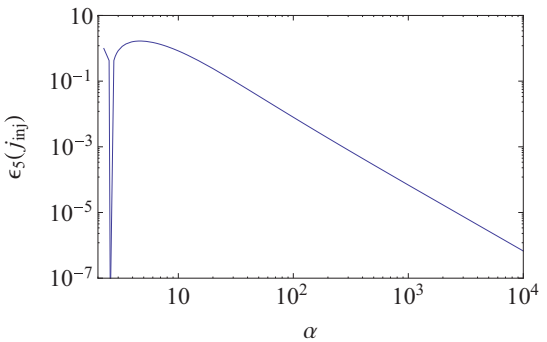

FIG. 7. Error $\epsilon_5(j_{\rm inj})$ vs α for the proposal (D9) with $k = m = \gamma = 1$ and $\mathcal{T} = 1/3$.

IV. CONCLUSION

Summarizing, this work has analyzed the dissipated and injected power distributions of an effective nonlinear damped massive system subject to an athermal dichotomous reservoir, i.e., the interaction between the system and the reservoir is defined by the telegraph noise that is alternately equal to $\pm a$ for average spells of $2/\alpha$, with α being the color of the noise. Mechanically, this system absolutely corresponds to the standard case from which nonequilibrium relations have been either found or illustrated. Thermomechanically, systems of this ilk are employed to describe a large variety of phenomena from physical to physiological and where the present results are expected to be probed. In analytical terms, this model is known for not bearing closed solutions to the position and velocity, a handicap that naturally extends to thermostatistical quantities as well.

Computing the statistical moments directly from the dynamical equation, one has set forth ansatz distributions for the dissipated and injected power $p(j_{\rm dis})$ and $p(j_{\rm inj})$. The former is derived from $p(v)$ and has a maximal error of 0.2% in $\langle j_{\rm dis}^4\rangle$, whereas for the injected power the error is never larger than 1.7% in $\langle j_{\rm inj}^5\rangle$. The latter can be further improved at the expense of an increase of the complexity of the solution by imposing the match in $\langle j_{\rm inj}^5\rangle$ (the last free parameter), yet such tweaking will not essentially change the functional and qualitative behavior of the curve, especially the superexponential limit of the FR (see Appendix B). This procedure can be further used to compute the distribution of the work done in driving such a system from a steady state into another as well.

In the white-noise limit, the fluctuation relation of the injected power $\mathrm{FR}_{\alpha\to\infty}$ has the usual thermal form equal to $\exp[2\langle j_{\rm inj}\rangle|j_{\rm inj}|/\sigma^2_{j_{\rm inj}}]$; however, $p(j_{\rm inj})$ is utterly different from that case as it is a Gaussian distribution. This result is paradoxical since not even (linear) thermal reservoirs yield a Gaussian distribution for $p(j_{\rm inj})$. Recalling that the telegraph noise is always bimodal, we have learned that the Gaussian nature of the reservoir is irrelevant to obtaining the standard

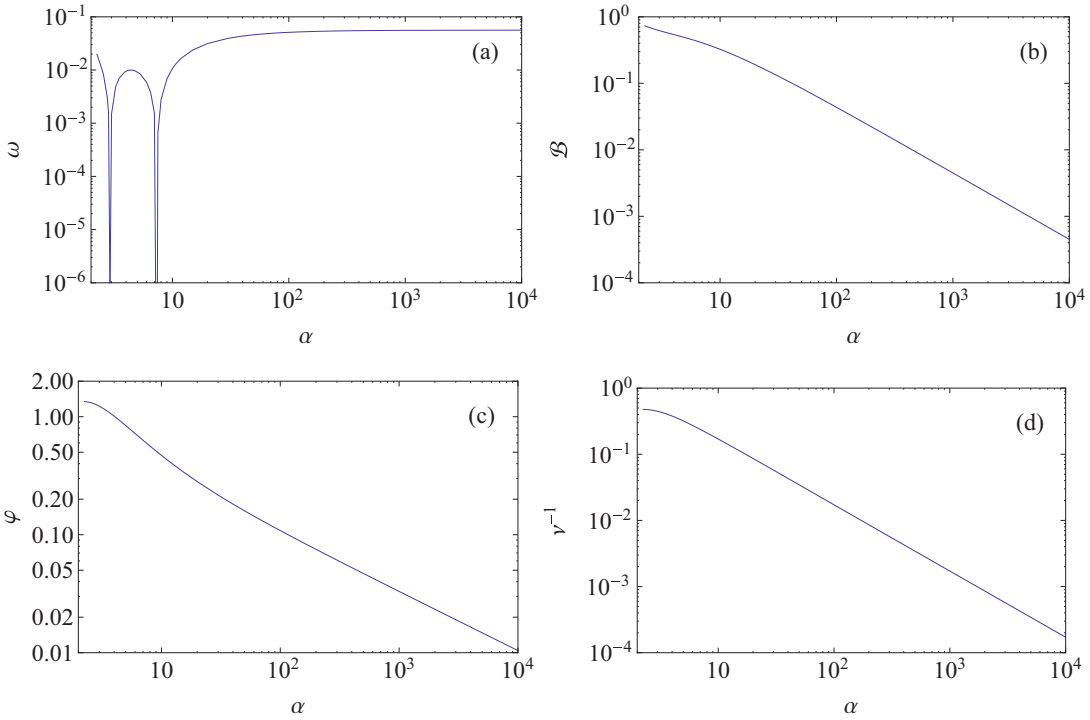

FIG. 8. Parameters (a) ω, (b) $\mathcal{B}$, (c) φ, and (d) ν vs α with $k = m = \gamma = 1$ and $\mathcal{T} = 1/3$.

FR; the key property is actually the infinite rate at which the values of the system-reservoir interaction update.

I have also revealed that for finite α, the fluctuation relation is clearly nonexponential and not even asymptotically converging, as it happens for Poissonian reservoirs, which like the thermal reservoir belongs to the Lévy-Itô class of stochastic processes. Due to the divergence from the second-order cumulant on, an asymptotically nonexponential form of the fluctuation relation is likely for Lévy particles [34], but it is surprising for a system where the physical observables have all of their cumulants finite and thus the standard FR is expected, at least in the large $j_{\rm inj}$ limit. With these results, we have also shown how defective the thermostatistical analysis of an athermal system can be if the results obtained for thermal processes abiding by the fluctuation-dissipation theorem are employed in a straightforward way.

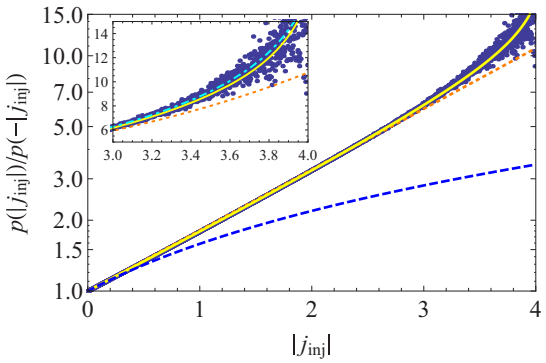

FIG. 9. The solid yellow line is the fluctuation relation obtained from Eq. (25) and the symbols show the numerical fluctuation relation for the same dynamical parameters $k = m = \gamma = 1$, $\mathcal{T} = 1/3$, and $\alpha = 10$. The dotted orange line is given by Eq. (23), which equals the standard (thermal) fluctuation relation, and the dashed blue line is the small $j_{\rm inj}$ asymptotic regime. In the inset, the dot-dashed cyan line corresponds to the fluctuation relation obtained according to the improvement discussed in Appendix B.

ACKNOWLEDGMENTS

This work benefited from financial support from FAPERJ (Grant No. APQ1-110.635/2014 and Jovem Cientista do Nosso Estado 202.881/2015) and CNPq (Grant No. 308737/2013-0).

APPENDIX A: METHOD OF SOLUTION FROM THE DYNAMICS

Let us define the Laplace-Fourier transform as

$$\widetilde{\mathcal{O}}(iq+\varepsilon) \equiv \lim_{\varepsilon\to 0}\int \mathcal{O}(t)e^{-(iq+\varepsilon)t}dt. \tag{A1}$$

The Fourier-Laplace transform of Eq. (2) is equal to

$$\begin{aligned} m(iq+\varepsilon)\tilde{v}(iq+\varepsilon) &= -\gamma\,\tilde{v}(iq+\varepsilon) - k\tilde{x}(iq+\varepsilon) \\ &\quad + \tilde{\zeta}(iq+\varepsilon), \\ \tilde{v}(iq+\varepsilon) &= (iq+\varepsilon)\tilde{x}(iq+\varepsilon). \end{aligned} \tag{A2}$$

Plugging the second line into the first one, we eliminate the velocity and we have for the position in reciprocal space

$$\tilde{x}(iq+\varepsilon) = \frac{\tilde{\zeta}(iq+\varepsilon)}{R(iq+\varepsilon)}. \tag{A3}$$

The function $R(s)$ reads

$$R(s) = m(s-\kappa_+)(s-\kappa_-), \tag{A4}$$

with its zeros located at

$$\kappa_\pm = -\frac{\theta}{2} \pm i\Omega = -\frac{\theta}{2} \pm i\sqrt{4\omega^2-\theta^2},$$

where

$$\theta = \frac{\gamma}{m}, \quad \omega^2 = \frac{k}{m}. \tag{A5}$$

The powers, namely, the dissipated

$$j_{\rm dis}(t) \equiv \gamma v(t)^2 \tag{A6}$$

and the injected

$$j_{\rm dis} \equiv \zeta(t)v(t), \tag{A7}$$

depend on the values of the velocity and the stochastic force. Both can be written as follows. Consider a generic quantity $\mathcal{O}(t)$ that in reciprocal space is recast as

$$\widetilde{\mathcal{O}}(iq_1+\varepsilon) = h(iq_1+\varepsilon)\tilde{x}(iq_1+\varepsilon). \tag{A8}$$

This means that for the velocity $h_v(s) = s$ and for the noise $h_\zeta(s) = R(s)$.

Since the system reaches a stationary state the ergodic property

$$\langle\mathcal{O}\rangle = \overline{\mathcal{O}} \equiv \lim_{\Xi\to\infty}\frac{1}{\Xi}\int \mathcal{O}(t)dt \tag{A9}$$

relating averages over samples $\langle\mathcal{O}\rangle$ and averages over time $\overline{\mathcal{O}}$ holds. Considering the final value theorem, we can connect the computation of statistics over time with the Laplace-Fourier transform

$$\overline{\mathcal{O}} = \lim_{\Xi\to\infty}\frac{1}{\Xi}\int \mathcal{O}(t)dt = \lim_{z\to 0} z\int e^{-zt}\mathcal{O}(t)dt. \tag{A10}$$

Using Eq. (A1) in Eq. (A10) as well as the equality between time and sample averaging in the stationary state, we get for the nth-order moment

$$\langle\mathcal{O}^n\rangle = \lim_{z\to 0,\varepsilon\to 0} \times\int \frac{z}{z-\sum_{l=1}^n(iq_l+\varepsilon)}\frac{h(iq_1+\varepsilon)\cdots h(iq_n+\varepsilon)}{R(iq_1+\varepsilon)\cdots R(iq_n+\varepsilon)} \times\langle\tilde{\zeta}(iq_1+\varepsilon)\cdots\tilde{\zeta}(iq_n+\varepsilon)\rangle\frac{dq_1}{2\pi}\cdots\frac{dq_n}{2\pi}. \tag{A11}$$

The multiple integration in $q_1,\ldots,q_n$ eliminates all the modes related to the transient. Analytically, this means that only combinations of poles that lead to a final expression proportional to z/z yield an *a priori* nonvanishing solution. Only terms proportional to $[\sum_{l=1}^{\ell}(iq_l+\varepsilon)]^{-1}$ are in agreement with that condition. From $R(q)$, those terms arise from the moments of the noise $\langle\tilde{\zeta}(iq_1+\varepsilon)\cdots\tilde{\zeta}(iq_n+\varepsilon)\rangle$.

Moments of ζ. The general form of the nth-order moments of ζ are quite intricate, but taking into consideration the symmetric properties of the telegraph noise assumed in this work, the $2n$-order moment of ζ is equal to

$$\langle\zeta(t_1)\cdots\zeta(t_{2n})\rangle = a^{2n}\exp\left[-\alpha\sum_{l=1}^{n}(t_{2l-1}-t_{2l})\right], \quad t_1 > \ldots > t_{2n}, \tag{A12}$$

whose Laplace-Fourier transform reads

$$\langle\tilde{\zeta}(iq_1+\varepsilon)\cdots\tilde{\zeta}(iq_{2n}+\varepsilon)\rangle = \frac{a^{2n}}{\prod_{l=1}^{n}\left[\sum_{o=1}^{2l}(iq_o+\varepsilon)\right]\prod_{l'=1}^{n}\left[\alpha+\sum_{o=1}^{2l'-1}(iq_o+\varepsilon)\right]}, \tag{A13}$$

where the first product contains the terms that give rise to nonvanishing contributions of the long-term moments.

APPENDIX B: TENTATIVE IMPROVEMENT TO EQ. (25)

Despite the quality of the approach conveyed in the main text, especially when one takes into account that it arises from a quantity $p(v)$, for which there is no closed solution, the results can be further improved by taking into consideration the analysis of $p(v)$. As stated, the major impact of letting δ assume values different from 2 corresponds to a more accurate determination of the minimal and maximal values of the injected power distribution

$$p(j_{\rm inj}) = \frac{1}{\mathcal{N}}\left[1-\frac{\mathcal{B}}{v}|j'_{\rm inj}|^\delta\right]^v \times \begin{cases} \frac{1}{\eta(-\mathcal{B})^{1/\delta}}B_{-\frac{v}{\mathcal{B}|\varphi j'_{\rm inj}|^\delta}}\left[v-\frac{1}{\delta},1-v\right] \Leftarrow j_{\rm inj} < \omega \\ \left(\frac{v}{\mathcal{B}}\right)^{1/\delta}\frac{\Gamma\left[1+\frac{1}{\delta}\right]\Gamma\left[v-\frac{1}{\delta}\right]}{\Gamma[v]} + \varphi j'_{\rm inj}\,{}_2F_1\left[\frac{1}{\delta},v;1+\frac{1}{\delta};-\frac{\mathcal{B}}{v}|\varphi(j'_{\rm inj})^\delta|\right] \Leftarrow j_{\rm inj} \geqslant \omega, \end{cases} \tag{B1}$$

where $j'_{\rm inj} \equiv j_{\rm inj} - \omega$, $B_{b_1}[b_2,b_3]$ is the Beta function, and $-(v/\mathcal{B})^{1/\delta}+\omega \leqslant j_{\rm inj} \leqslant (v/\mathcal{B})^{1/\delta}+\omega$.

As visible from Fig. 10, the cyan line [obtained by a nonlinear numerical adjustment of Eq. (B1) to the empirical distribution] permitting $\delta \neq 2$ broadens the distribution and increases the absolute value of its upper and lower bounds with. Nonetheless, it must be clearly emphasized that both the Beta function and the hypergeometric function decay as a power law for large values of $|j_{\rm inj}|$, which guarantees that the fluctuation relation preserves a nonexponential power-law functional dependence ($\delta = 2 \to \delta \neq 2$) along the lines I have asserted in Sec. III. That is patent in the inset of Fig. 9, which shows an improvement in the comparison with the numerical results; however, as expected, it does not introduce drastic changes and the conclusions that can be obtained from both approaches are qualitatively the same.

APPENDIX C: STATIONARY DISTRIBUTIONS OF v AND $j_{\rm inj}$ IN THE QUASIDETERMINISTIC CASE $\alpha < \gamma/m$

Under this condition, the time the stochastic force takes to change its sign is larger than the typical scale of relaxation. Because of that, one considers ζ constant and the determinist solution to Eq. (2) with the initial conditions $x(0) = x_0$ and $v(0) = v_0$ is equal to

$$x(t) = \exp\left[-\frac{\gamma}{2m}t\right]\left(\frac{2km v_0+\gamma k x_0-\gamma\xi}{km\Omega}\sin\left[\frac{\Omega}{2}t\right]+\frac{kx_0-\xi}{k}\cos\left[\frac{\Omega}{2}t\right]\right)+\frac{\xi}{k} \tag{C1}$$

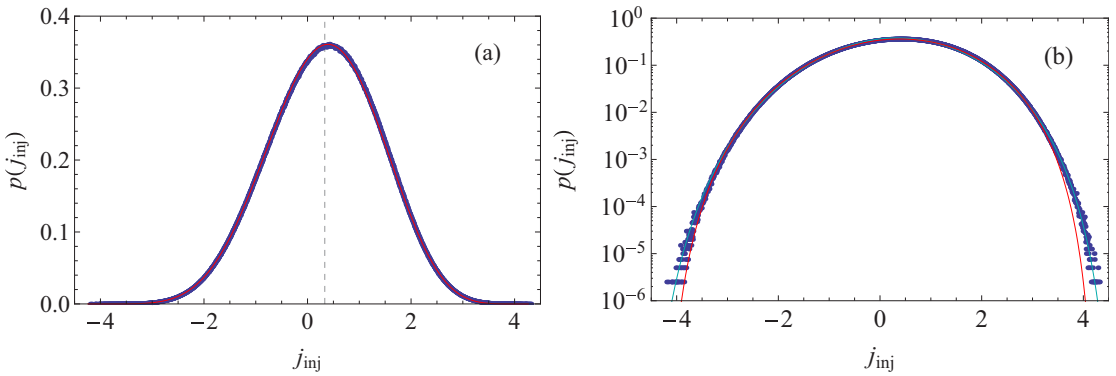

FIG. 10. Blue symbols represent the empirical distribution function obtained from the dynamics (2) with $m = k = \gamma = 1$ and $\mathcal{T} = 1/3$; the red line is Eq. (25) obtained with moment matching with $\omega = 0.1065\ldots$, $\mathcal{B} = 0.3249\ldots$, $\varphi = 0.4704\ldots$, and $\nu = 5.8804\ldots$; and the cyan line is Eq. (B1) obtained from numerical adjustment with $\omega = 0.1056 \pm 0.0003$, $\mathcal{B} = 0.3837 \pm 0.0004$, $\varphi = 0.425 \pm 0.002$, $\nu = 6.74 \pm 0.05$, and $\delta = 2.08 \pm 0.02$ in (a) lin-lin and (b) log-lin scales. The dashed line in (a) represents the average values $\langle j_{\rm inj}\rangle = 1/3$. The plot shows that the average value is different from the mode of the distribution.

and the velocity reads

$$v(t) = \exp\left[-\frac{\gamma}{2m}t\right] \times \left\{\frac{m^2\Omega^2(\xi - kx_0) + \gamma[\gamma\xi - k(2mv_0 + \gamma x_0)]}{2km^2\Omega} \times \sin\left[\frac{\Omega}{2}t\right] + v_0\cos\left[\frac{\Omega}{2}t\right]\right\}. \quad \text{(C2)}$$

The first zero of the velocity occurs at

$$t_z = \frac{2\pi}{\Omega}. \quad \text{(C3)}$$

At this instant, it is possible to verify that the position reaches a local extreme.

The velocity has local maxima at

$$t_{v_{\max}} = \frac{2\arctan\left[\frac{-\gamma/m \pm \sqrt{(\gamma/m)^2 + \Omega^2}}{\Omega}\right] + 2\pi n}{\Omega/2}, \quad n \in \mathbb{N}, \quad \text{(C4)}$$

with the respective values being obtained by plugging Eq. (C4) into Eq. (C2). In ascending order, we have $t^{(+)}_{v_{\max}}(n=0) < t^{(-)}_{v_{\max}}(n=1) < t^{(+)}_{v_{\max}}(n=1) < t^{(-)}_{v_{\max}}(n=2) < \cdots$, which relate to the values $\{v_1^{\max}, v_2^{\max}, v_3^{\max}, \ldots\}$, respectively.

For a system evolving according to a simple sinusoidal function $u = u(t)$, it is known that the distribution of u goes as a Beta distribution

$$p(u) \propto \frac{1}{\sqrt{4u_{\max}^2 - u^2}}. \quad \text{(C5)}$$

One must now take into consideration that owing to damping, there is a set of local maxima and thus the distribution will be given by a superposition of distributions $p(u)$ with different values of $u^2_{\max}$. If α is not dramatically less than γ/m, then the particle is likely to experience a change in the value of ζ before it reaches the stable solution $v_\infty = 0$ and $x_\infty = \xi/k$. If that change occurs when $|x(t)|$ is larger than the asymptotic position ζ/k, then the maximal speed achieved by the particle can be larger than the maximal speed obtained for $x(0) = v(0) = 0$. Putting it into figures, if ζ flips into $-\zeta$ within a time

$$\frac{4}{\Omega}\arctan\left[\frac{\gamma + \sqrt{\gamma^2 + m^2\Omega^2}}{m\Omega}\right] < t < \frac{4}{\Omega}\left(\arctan\left[\frac{\gamma + \sqrt{\gamma^2 + m^2\Omega^2}}{m\Omega}\right] + \pi\right), \quad \text{(C6)}$$

we can have a surge in the maximal speed $|v_1^{\max}|$.

For the parameters I have considered, one verifies that the maximal speed is attained after the fourth flip, with the maximal value after the fifth ζ change yielding a small $|v_1^{\max}|$. In Fig. 11 one can see that the maximal of the four flips is not attained, a fact that is easily explained by taking into account that the interevent probability $Q(t)$ of a symmetric telegraph noise with color α is the value $Q(t) = (\alpha/2)\exp[-\alpha t/2]$, the probability of having at $t_{v_{\max}} \pm 1\%$ is of the order of $\alpha/4$, and the probability of having a flip in ζ in the interval described by Eq. (C6) is $5\alpha/4$. Therefore, the first number gets extremely low in the quasideterministic regime. Nevertheless, taking into account the form of $Q(t)$ [on which $p(v)$ for large values of v hinges] and the number of flips needed to reach maximal speed η, we estimate that the distribution of the velocity decays close to

$$f_{\rm tail}(v) \sim \exp\left[-\frac{|v|}{\mathcal{V}}\right], \quad |v_1^{\max}| < v < \widetilde{v^{\max}}, \quad \text{(C7)}$$

where $\widetilde{v^{\max}}$ is the average of the maximal values of the velocity above $|v_1^{\max}|$ and $\mathcal{V}$ has velocity dimensions (length)$\times$(time)$^{-1}$ and is naturally a function of the parameters of the problem. Under this rubric one estimates

$$\mathcal{V} = \left[\frac{\gamma\xi}{km\Omega}\right]\left[\eta\frac{\alpha}{2}\right], \quad \text{(C8)}$$

which is concurrent with the numerical analysis shown in the inset of Fig. 11. From this whole reasoning we have

$$p(v) \approx \frac{1}{\eta + Z}\left[\delta(v) + \sum_{i=1}^{\eta-2}\frac{1}{\pi\sqrt{\left(2v_i^{\max}\right)^2 - v^2}} + f_{\rm tail}(v)\right], \quad \text{(C9)}$$

where $Z = \int f_{\rm tail}(v)dv$.

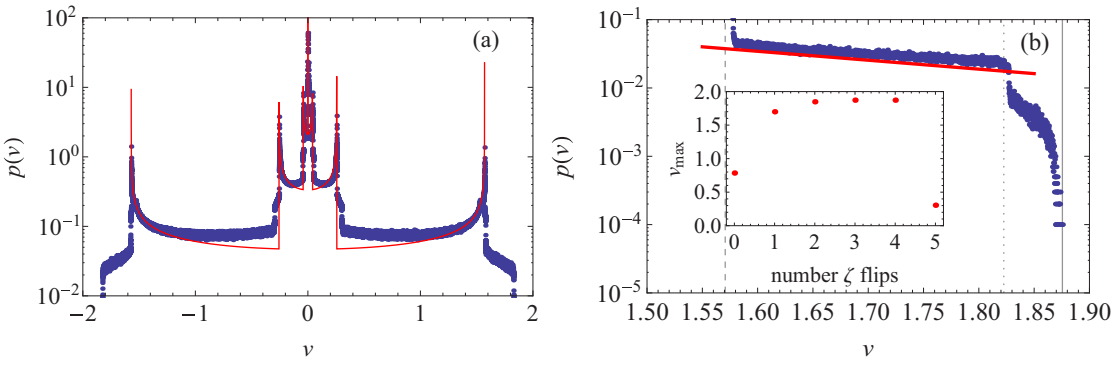

FIG. 11. (a) Distribution $p(v)$ vs v for $m = k = \gamma = 1$, $\mathcal{T} = 1/3$, and $\alpha = 1/5$. (b) Close-up of the behavior after $|2v_1^{\max}|$ and the maximal velocity that was computed at $1.8755\ldots$ (vertical line). The red line has slope $\mathcal{V}^{-1} = 3.01\ldots$ as obtained by the parameters. The slump indicated by the dotted line is located at $v \simeq 2.62$, which corresponds to the average of the maximal values of the velocity above $|v_1^{\max}|$, $\widetilde{v^{\max}}$. The inset shows the maximal speed given by the number of flips of ζ if that flip occurs at maximal displacement from ζ/k.

With respect to the injected power, it is intuitive to think that $p(j_{\rm inj})$ is built upon $p(v)$ and taking into consideration that $j_{\rm inj} = v(t)\eta(t)$. On that account, we comprehend that the component of the injected power distribution is associated with $v_2^{\max}$ [which is actually a local minimum (assuming $\zeta > 0$)] and must be centered on negative value. Assuming that $p(j_{\rm inj})dj_{\rm inj} = p(v)dv$, the bulk of the distribution is given by the superposition of

$$p_i(j_{\rm inj}) \sim \frac{1}{\sqrt{\left(\xi v_i^{\max}\right)^2 - \left(j_{\rm inj} - \xi v_i^{\max}\right)^2}}. \qquad \text{(C10)}$$

The postbulk part of the distribution before the real tail exhibits an exponential decay with a slope $(\xi\mathcal{V})^{-1}$ for the positive side and $(2\xi\mathcal{V})^{-1}$ for the negative part of the distribution. A comparison is shown in Fig. 12. It is visible that the extreme tails of the distribution of the injected power decays much faster than the exponential.

APPENDIX D: EXPLICIT RELATIONS FOR THE MOMENTS

In this Appendix the dynamical statistical moments of the quantity $\mathcal{O}$ are denoted by $\langle\mathcal{O}\rangle$ and the probability cumulant by $\langle\mathcal{O}\rangle_p$.

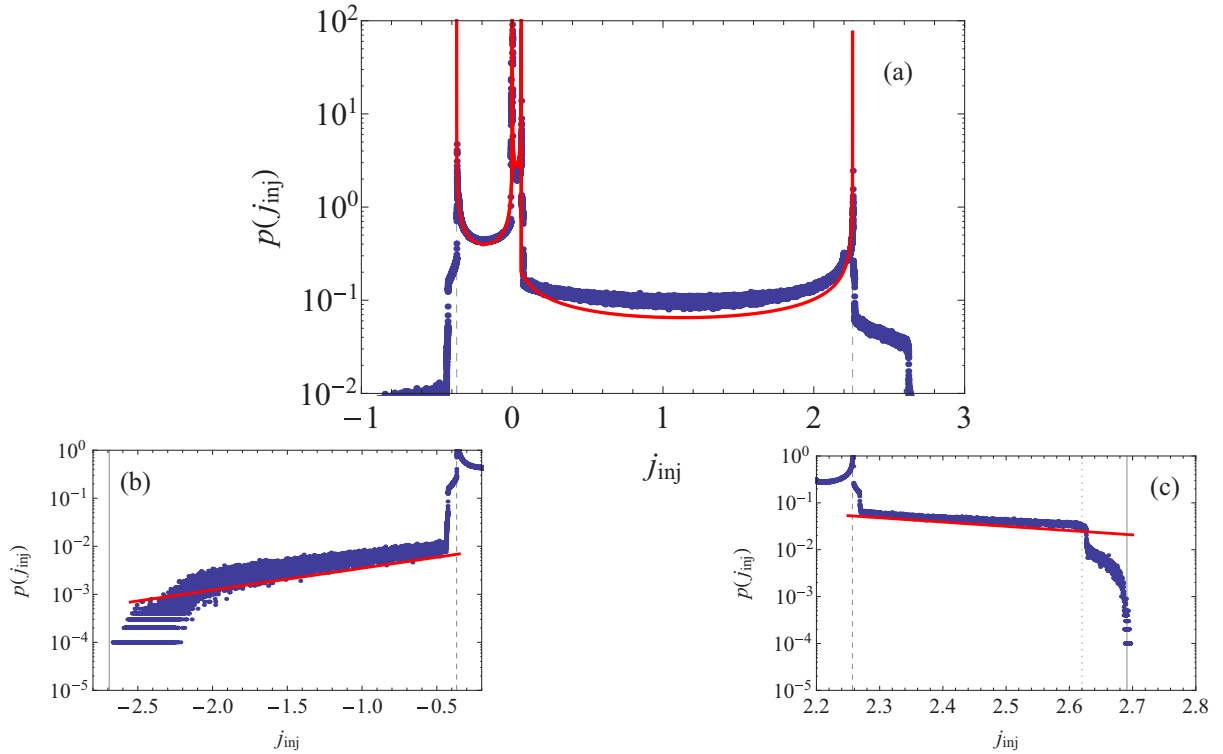

FIG. 12. (a) Distribution of the injected power for $m = k = \gamma = 1$, $\mathcal{T} = 1/3$, and $\alpha = 1/5$. Also shown are close-ups of the behavior (b) before $-2\xi|v_2^{\max}| = -0.3680\ldots$ and (c) after $2\xi|v_1^{\max}| = 2.257\ldots$ and the maximal injected power equal to $\pm 2.691\ldots$. (b) and (c) also show the pretail decays that in this case are close to exponentials with both slopes indicated in the text.

1. Moments of the velocity

a. Formulas obtained from Eq. (2)

The second- and fourth-order dynamical moments were obtained in [32] for generic cases and for our fully symmetrical conditions they amount to

$$\langle v^2\rangle = \frac{a^2\alpha}{\gamma\hat{k}} = \frac{\mathcal{T}}{m} \tag{D1}$$

and

$$\langle v^4\rangle = \frac{3a^4\alpha}{\gamma^2(4km+3\gamma^2)\Psi}\left[18k^2m(2\hat{\gamma}-\gamma)+3\alpha\gamma^2\hat{\gamma}(\hat{\gamma}+\gamma)+k\left(4\delta_\gamma^3+14\delta_\gamma^2\gamma+49\delta_\gamma\gamma^2+36\gamma^3\right)\right], \tag{D2}$$

with

$$\delta_{\mathcal{O}} \equiv \hat{\mathcal{O}} - \mathcal{O}, \tag{D3}$$

$$\Psi \equiv \hat{k}\alpha - \gamma, \tag{D4}$$

$$\Phi \equiv \gamma^3(km+2\gamma^2)(16km+5\gamma^2)[km+(\hat{\gamma}+\gamma)(\hat{\gamma}+2\gamma)][9km+\hat{\gamma}(\hat{\gamma}+3\gamma)][25k+\alpha(\hat{\gamma}+4\gamma)], \tag{D5}$$

$$\begin{aligned}\Upsilon \equiv{}& \gamma(4km+3\gamma^2)(36km+7\gamma^2)(4km+15\gamma^2)[km+(\hat{\gamma}+2\gamma)(\hat{\gamma}+3\gamma)]\\ &\times[49k+\alpha(\hat{\gamma}+6\gamma)][9km+(\hat{\gamma}+\gamma)(\hat{\gamma}+4\gamma)][25km+\hat{\gamma}(\hat{\gamma}+5\gamma)].\end{aligned} \tag{D6}$$

The sixth-order moment, which together with the previous two is need to obtain the values of the parameters $\mathcal{B}$, ν, and δ, and the eighth-order moment, which is used to appraise the quality of the approximation, are especially computed for this case and they are equal to

$$\begin{aligned}\langle v^6\rangle = {}& \frac{15a^6\alpha}{\gamma^3(4km+3\gamma^2)\Psi\Phi}\left[30\alpha^2\gamma^6\hat{\gamma}^2(\hat{\gamma}+\gamma)^2(\hat{\gamma}+2\gamma)(6\hat{\gamma}+3\gamma)+7200k^6m^4(6\hat{\gamma}+5\gamma)(3\hat{\gamma}-\gamma)\right.\\ &+2k^5m^3\left(132400\gamma^4+662471\gamma^3\delta_\gamma+436066\gamma^2\delta_\gamma^2+96048\gamma\delta_\gamma^3+16992\delta_\gamma^4\right)\\ &+k^4m^2\left(630400\gamma^6+1717572\gamma^5\delta_\gamma+1677781\gamma^4\delta_\gamma^2+847182\gamma^3\delta_\gamma^3+225164\gamma^2\delta_\gamma^4+27296\gamma\delta_\gamma^5+2752\delta_\gamma^6\right)\\ &+k^3m\left(489600\gamma^8+1607864\gamma^7\delta_\gamma+2062358\gamma^6\delta_\gamma^2+1299041\gamma^5\delta_\gamma^3+455517\gamma^4\delta_\gamma^4+101202\gamma^3\delta_\gamma^5+14348\gamma^2\delta_\gamma^6\right.\\ &\left.+928\gamma\delta_\gamma^7+64\delta_\gamma^8\right)+k^2\gamma^2\left(115200\gamma^8+487536\gamma^7\delta_\gamma+820244\gamma^6\delta_\gamma^2+729262\gamma^5\delta_\gamma^3+384501\gamma^4\delta_\gamma^4+123904\gamma^3\delta_\gamma^5\right.\\ &\left.+23871\gamma^2\delta_\gamma^6+2770\gamma\delta_\gamma^7+196\delta_\gamma^8\right)+k^2\gamma^2\left(115200\gamma^8+487536\gamma^7\delta_\gamma+820244\gamma^6\delta_\gamma^2\right.\\ &\left.+729262\gamma^5\delta_\gamma^3+384501\gamma^4\delta_\gamma^4+123904\gamma^3\delta_\gamma^5+23871\gamma^2\delta_\gamma^6+2770\gamma\delta_\gamma^7+196\delta_\gamma^8\right)\\ &\left.+k\alpha\gamma^4\hat{\gamma}(\hat{\gamma}+\gamma)\left(12960\gamma^5+28116\gamma^4\delta_\gamma+20576\gamma^3\delta_\gamma^2+7559\gamma^2\delta_\gamma^3+1570\gamma\delta_\gamma^4+151\delta_\gamma^5\right)\right]\end{aligned} \tag{D7}$$

and

$$\begin{aligned}\langle v^8\rangle = {}& \frac{105a^8\alpha}{\gamma^3(4km+3\gamma^2)\Psi\Phi\Upsilon}\left[9450\alpha^3\gamma^{12}\hat{\gamma}^3(\hat{\gamma}+\gamma)^3(\hat{\gamma}+2\gamma)^2(\hat{\gamma}+3\gamma)^2(\hat{\gamma}+4\gamma)(\hat{\gamma}+5\gamma)\right.\\ &+22861440000m^9k^{12}\left(3\gamma^3+108\gamma\delta_\gamma^2+59\gamma^2\delta_\gamma+36\alpha^3\right)\\ &+129600m^8k^{11}\left(13154883\gamma^5+205825503\gamma^4\delta_\gamma+321906444\gamma^3\delta_\gamma^2+130746580\gamma^2\delta_\gamma^3+22802688\gamma\delta_\gamma^4+2754432\delta_\gamma^5\right)\\ &+144m^7k^{10}\left(101869879125\gamma^7+1113351239214\gamma^6\delta_\gamma+1513670232684\gamma^5\delta_\gamma^2+861920233464\gamma^4\delta_\gamma^3\right.\\ &\left.+282590656896\gamma^3\delta_\gamma^4+54830216096\gamma^2\delta_\gamma^5+5755242240\gamma\delta_\gamma^6+421445376\delta_\gamma^7\right)+4m^6k^9\left(14585447104200\gamma^9\right.\\ &+107718183204455\gamma^8\delta_\gamma+16986540517052\gamma^7\delta_\gamma^2+1256655428924 72\gamma^6\delta_\gamma^3+53594657126928\gamma^5\delta_\gamma^4\\ &\left.+1450624950344 0\gamma^4\delta_\gamma^5+267089164588 8\gamma^3\delta_\gamma^6+33245964000 0\gamma^2\delta_\gamma^7+24467816448\gamma\delta_\gamma^8+1275826176\delta_\gamma^9\right)\\ &+4m^5k^8\left(30772809597600\gamma^{11}+162623360141110\gamma^{10}\delta_\gamma+28603717096559 9\gamma^9\delta_\gamma^2+26096274021006 6\gamma^8\delta_\gamma^3\right.\\ &+14557029732827 6\gamma^7\delta_\gamma^4+5372764931413 6\gamma^6\delta_\gamma^5+1355485130388 8\gamma^5\delta_\gamma^6+236631559027 2\gamma^4\delta_\gamma^7\\ &\left.+29250131788 8\gamma^3\delta_\gamma^8+2559979571 2\gamma^2\delta_\gamma^9+137466777 6\gamma\delta_\gamma^{10}+55213056\delta_\gamma^{11}\right)+m^4k^7\left(146079614419200\gamma^{13}\right.\\ &\left.+67332495041328 0\gamma^{12}\delta_\gamma+12989373014604 88\gamma^{11}\delta_\gamma^2+13989871416509 53\gamma^{10}\delta_\gamma^3+94957341478076 8\gamma^9\delta_\gamma^4\right.\\ &\left.+43432371586058 0\gamma^8\delta_\gamma^5+13968752475377 6\gamma^7\delta_\gamma^6+3248095916662 4\gamma^6\delta_\gamma^7+551141462252 8\gamma^5\delta_\gamma^8\right.\end{aligned}$$

$$
\begin{aligned}
&+674661522496\gamma^4\delta_\gamma^9+59244718336\gamma^3\delta_\gamma^{10}+3740824320\gamma^2\delta_\gamma^{11}+143179776\gamma\delta_\gamma^{12}+4644864\delta_\gamma^{13}\big)\\
&+2m^3k^6\big(49444684329600\gamma^{15}+242847778998240\gamma^{14}\delta_\gamma+518054563964592\gamma^{13}\delta_\gamma^2+634395072125717\gamma^{12}\delta_\gamma^3\\
&+501682141266615\gamma^{11}\delta_\gamma^4+273588627177923\gamma^{10}\delta_\gamma^5+107023373036174\gamma^9\delta_\gamma^6+30713177257768\gamma^8\delta_\gamma^7\\
&+6543676765560\gamma^7\delta_\gamma^8+1042329832784\gamma^6\delta_\gamma^9+124083645600\gamma^5\delta_\gamma^{10}+10805855936\gamma^4\delta_\gamma^{11}\\
&+668781568\gamma^3\delta_\gamma^{12}+29622528\gamma^2\delta_\gamma^{13}+681984\gamma\delta_\gamma^{14}+18432\delta_\gamma^{15}\big)\\
&+m^2k^5\gamma^2\big(37261556236800\gamma^{15}+206348951397312m\gamma^{14}\delta_\gamma+502526596906944\gamma^{13}\delta_\gamma^2+713526202827144\gamma^{12}\delta_\gamma^3\\
&+661967396039776\gamma^{11}\delta_\gamma^4+426819773462303\gamma^{10}\delta_\gamma^5+198730218933658\gamma^9\delta_\gamma^6+68523162500403\gamma^8\delta_\gamma^7\\
&+17774322400960\gamma^7\delta_\gamma^8+3490331685988\gamma^6\delta_\gamma^9517126851280\gamma^5\delta_\gamma^{10}+57265238304\gamma^4\delta_\gamma^{11}+4682031040\gamma^3\delta_\gamma^{12}\\
&+272837312\gamma^2\delta_\gamma^{13}+10497280\gamma\delta_\gamma^{14}+285952\delta_\gamma^{15}\big)+2mk^4\gamma^4\big(3593818368000\gamma^{15}+23720294612160\gamma^{14}\delta_\gamma\\
&+68508160820064\gamma^{13}\delta_\gamma^2+115161863097096\gamma^{12}\delta_\gamma^3+126561745923096\gamma^{11}\delta_\gamma^4+96923640848279\gamma^{10}\delta_\gamma^5\\
&+53802181256450\gamma^9\delta_\gamma^6+22189228510173\gamma^8\delta_\gamma^7+6897533455102\gamma^7\delta_\gamma^8+1626983860750\gamma^6\delta_\gamma^9\\
&+291452948250\gamma^5\delta_\gamma^{10}+39413861188\gamma^4\delta_\gamma^{11}+3951209848\gamma^3\delta_\gamma^{12}+282915600\gamma^2\delta_\gamma^{13}+13637984\gamma\delta_\gamma^{14}+376448\delta_\gamma^{15}\big)\\
&+k^3\gamma^6\big(548674560000\gamma^{15}+4947931008000\gamma^{14}\delta_\gamma+18403154847360\gamma^{13}\delta_\gamma^2+38648225054736\gamma^{12}\delta_\gamma^3\\
&+32398743082888\gamma^9\delta_\gamma^6+15989498629087\gamma^8\delta_\gamma^7+52153135324704\gamma^{11}\delta_\gamma^4+48484670606232\gamma^{10}\delta_\gamma^5\\
&+5927517027284\gamma^7\delta_\gamma^8+1664923361414\gamma^6\delta_\gamma^9+354472762668\gamma^5\delta_\gamma^{10}+56701607823\gamma^4\delta_\gamma^{11}\\
&+6679340096\gamma^3\delta_\gamma^{12}+558513308\gamma^2\delta_\gamma^{13}+30637648\gamma\delta_\gamma^{14}+862048\delta_\gamma^{15}\big)\\
&+6k^2\alpha\gamma^8\hat{\gamma}(\hat{\gamma}+\gamma)\big(11648448000\gamma^{12}+62953977600\gamma^{11}\delta_\gamma+144335339640\gamma^{10}\delta_\gamma^2+188290456740\gamma^9\delta_\gamma^3\\
&+158039773770\gamma^8\delta_\gamma^4+91004188981\gamma^7\delta_\gamma^5+37204890166\gamma^6\delta_\gamma^6++10971829581\gamma^5\delta_\gamma^7\\
&+2339446461\gamma^4\delta_\gamma^8+356375064\gamma^3\delta_\gamma^9+37395639\gamma^2\delta_\gamma^{10}+2460974\gamma\delta_\gamma^{11}+77264\delta_\gamma^{12}\big)\\
&+45k\alpha^2\gamma^{10}\hat{\gamma}^2(\hat{\gamma}+\gamma)^2(\hat{\gamma}+2\gamma)^2(\hat{\gamma}+3\gamma)\big(1814400\gamma^6+4295280\gamma^5\delta_\gamma+3526828\gamma^4\delta_\gamma^2+1464672\gamma^3\delta_\gamma^3\\
&+348205\gamma^2\delta_\gamma^4+45354\gamma\delta_\gamma^5+2473\delta_\gamma^6\big)\big]. \qquad \text{(D8)}
\end{aligned}
$$

b. Formulas obtained from the ansatz

The even moments of distribution (D9),

$$p(v)=\frac{1}{\mathcal{Z}}\left[1-\frac{\mathcal{B}}{\nu}|v|^\delta\right]^\nu, \qquad \text{(D9)}$$

are equal to

$$\langle v^{2n}\rangle_p=\left(\frac{\nu}{\mathcal{B}}\right)^{2n/\delta}\frac{\Gamma\left[\frac{2n+1}{\delta}\right]\Gamma\left[1+\frac{1}{\delta}+\nu\right]}{\Gamma\left[\frac{1}{\delta}\right]\Gamma\left[1+\frac{2n+1}{\delta}+\nu\right]},\quad n\in\mathbb{N}. \qquad \text{(D10)}$$

c. Excursus

Despite the fact that $p(|j_{\rm dis}|)$ does not permit the calculation of a FR because $j_{\rm dis}$ is nonpositive, one can determine a FR-like relation $p(|\tilde{j}_{\rm dis}|)/p(-|\tilde{j}_{\rm dis}|)$, where $\tilde{j}_{\rm dis}\equiv\ln\frac{|j_{\rm dis}|}{\langle j_{\rm dis}\rangle}=\ln\frac{m|j_{\rm dis}|}{\gamma\mathcal{T}}$. In this way, it is possible to compare the probability of having a large depletion of power with the probability of having a little dissipation, in dissipated power units. Since in the white-noise limit the distribution converges to the χ^2 distribution with one degree of freedom

$$p_{\rm WN}(|j_{\rm dis}|)=\sqrt{\frac{m}{2\pi\gamma\mathcal{T}|j_{\rm dis}|}}\exp\left[-\frac{m}{2\gamma\mathcal{T}}|j_{\rm dis}|\right], \qquad \text{(D11)}$$

that relation is

$$\frac{p_{\rm WN}(|\tilde{j}_{\rm dis}|)}{p_{\rm WN}(-|\tilde{j}_{\rm dis}|)}=\exp[|\tilde{j}_{\rm dis}|-\sinh(|\tilde{j}_{\rm dis}|)]. \qquad \text{(D12)}$$

Equation (D12) has two asymptotic limits

$$\begin{aligned}
\lim_{\tilde{j}_{\rm dis}\gg1}\frac{p_{\rm WN}(|\tilde{j}_{\rm dis}|)}{p_{\rm WN}(-|\tilde{j}_{\rm dis}|)}&=\exp\left[-\frac{1}{2}\exp[|\tilde{j}_{\rm dis}|]\right],\\
\lim_{\tilde{j}_{\rm dis}\ll1}\frac{p_{\rm WN}(|\tilde{j}_{\rm dis}|)}{p_{\rm WN}(-|\tilde{j}_{\rm dis}|)}&=1.
\end{aligned} \qquad \text{(D13)}$$

These last results mean that around the average $\tilde{j}_{\rm dis}=0$ one has a quite similar behavior on its left-hand and right-hand sides. When comparing large dissipation with no dissipation, the first asymptotic limit of Eq. (D13) shows that the probability of the latter is overwhelmingly larger than that of the former. This feature is largely established by the exponential decay of the χ^2 distribution.

For finite values of α, a similar approach can be carried out, using Eq. (D9) though. However, natural differences emerge. First, we have the question related to the cutoff imposed by the compact support of Eq. (D9) and second, because of the nonexponential form $p(|j_{\rm dis}|)$, the FR-like relation for the

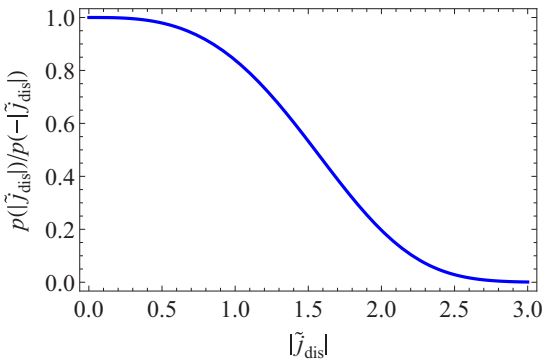

FIG. 13. Fluctuation relation for the logarithm of the absolute value of the dissipated power $\tilde{j}_{\rm dis}$ in the white-noise limit with $m = k = \gamma = 1$ and $\mathcal{T} = 1/3$.

logarithm of the dissipated power does not have a simple form, but it certainly does not have an (asymptotic) exponential form, but for intermediate values the FR-like relation decays more slowly because of the nonexponential features (see Fig. 13).

2. Moments of the injected power

a. Analytical and ansatz moments up to fourth order

Regarding $j_{\rm inj}$, one has for the average

$$\langle j_{\rm inj}\rangle = \frac{\gamma}{m}\mathcal{T}, \tag{D14}$$

for second order

$$\langle j_{\rm inj}^2\rangle = \frac{\alpha\gamma\hat{k}}{\delta_\gamma^2}\mathcal{T}^2, \tag{D15}$$

for third order

$$\langle j_{\rm inj}^3\rangle = 3\alpha\gamma^2\hat{k}^3\frac{\alpha\hat{\gamma}(\gamma+\hat{\gamma})+k(8\gamma+9\hat{\gamma})}{\delta_\gamma^3\Lambda}\mathcal{T}^3, \tag{D16}$$

and for fourth order

$$\langle j_{\rm inj}^4\rangle = 3\alpha\gamma^2\hat{k}^4\frac{3\alpha\gamma^2\hat{\gamma}(\gamma+\hat{\gamma})+18k^2m(2\hat{\gamma}-\gamma)+k\left(36\gamma^3+49\gamma^2\delta_\gamma+14\gamma\delta_\gamma^2+4\delta_\gamma^3\right)}{\Lambda\delta_\gamma^4(3\gamma^2+4km)}\mathcal{T}^4. \tag{D17}$$

The moments given by the ansatz (25),

$$p(j_{\rm inj}) = \left[1-\frac{\mathcal{B}}{\nu}(j_{\rm inj}-\omega)^2\right]^\nu\left\{\mathcal{A}+\varphi(j_{\rm inj}-\omega)\mathcal{A}'\right.$$
$$\left.\times{}_2F_1\left[\frac{1}{2},\nu;\frac{3}{2};-\frac{\mathcal{B}\alpha^2}{\nu}(j_{\rm inj}-\omega)^2\right]\right\},$$

where

$$\mathcal{A}\equiv\sqrt{\frac{\mathcal{B}}{\pi\nu^3}}\frac{\Gamma\left(\frac{3}{2}+\nu\right)}{\Gamma(\nu)},\quad \mathcal{A}'\equiv\frac{2\mathcal{B}\Gamma\left(\frac{3}{2}+\nu\right)}{\pi\nu^2\Gamma\left(\nu-\frac{1}{2}\right)}, \tag{D18}$$

read as follows: For the average

$$\langle j_{\rm inj}\rangle_p = \omega+\sqrt{\frac{\nu}{\pi\mathcal{B}}}\alpha\left(\nu^2-\frac{1}{4}\right)\Gamma[\nu]\,{}_2\tilde{F}_1\left[\frac{1}{2},\nu;\nu+\frac{5}{2};-\alpha^2\right]$$
$$= \omega+\langle j_{\rm inj}\rangle'_p, \tag{D19}$$

for second order

$$\left\langle j_{\rm inj}^2\right\rangle_p = \frac{\nu}{\mathcal{B}(2\nu+3)}+\omega(2\langle j_{\rm inj}\rangle'_p+\omega)$$
$$= \left\langle j_{\rm inj}^2\right\rangle'_p+\omega(2\langle j_{\rm inj}\rangle'_p+\omega), \tag{D20}$$

for third order

$$\left\langle j_{\rm inj}^3\right\rangle_p = \frac{3}{4}\left(\frac{\nu}{\mathcal{B}}\right)^{3/2}\alpha\left(\nu^2-\frac{1}{4}\right)\Gamma[\nu]$$
$$\times\,{}_3\tilde{F}_2\left(\frac{1}{2},\frac{5}{2},\nu;\frac{3}{2},\nu+\frac{7}{2};-\alpha^2\right)$$
$$+3\left\langle j_{\rm inj}^2\right\rangle'_p\omega+3\langle j_{\rm inj}\rangle'_p\omega^2+\omega^3$$
$$= \left\langle j_{\rm inj}^3\right\rangle'_p+\omega\left[3\left(\left\langle j_{\rm inj}^2\right\rangle'_p+\left\langle j_{\rm inj}^2\right\rangle'_p\omega\right)+\omega^2\right], \tag{D21}$$

with

$$\delta_{\mathcal{O}}\equiv\hat{\mathcal{O}}-\mathcal{O}, \tag{D22}$$

$$\Lambda\equiv\hat{k}[km+\hat{\gamma}(\hat{\gamma}+\gamma)][9k+\alpha(\hat{\gamma}+2\gamma)], \tag{D23}$$

and for fourth order

$$\left\langle j_{\rm inj}^4\right\rangle_p = \frac{3\nu^2}{(4\nu^2+16\nu+15)\mathcal{B}^2}+4\left\langle j_{\rm inj}^3\right\rangle'_p\omega$$
$$+6\left\langle j_{\rm inj}^2\right\rangle'_p\omega^2+4\langle j_{\rm inj}\rangle'_p\omega^3+\omega^4$$
$$= \left\langle j_{\rm inj}^4\right\rangle'_p+4\left\langle j_{\rm inj}^3\right\rangle'_p\omega+6\left\langle j_{\rm inj}^2\right\rangle'_p\omega^2+4\langle j_{\rm inj}\rangle'_p\omega^3+\omega^4. \tag{D24}$$

The dependence of the skewness

$$\gamma_1(j_{\rm inj})\equiv\frac{\left\langle\left\langle j_{\rm inj}^3\right\rangle\right\rangle}{\left\langle\left\langle j_{\rm inj}^2\right\rangle\right\rangle^{3/2}} \tag{D25}$$

and the kurtosis

$$\gamma_2(j_{\rm inj})\equiv\frac{\left\langle\left\langle j_{\rm inj}^4\right\rangle\right\rangle}{\left\langle\left\langle j_{\rm inj}^2\right\rangle\right\rangle^2} \tag{D26}$$

of injected power on α is depicted in Fig. 6.

b. Fifth-order moment error analysis

For the assessment of the approach, we compute the fifth-order moment as well, which for this probability distribution function is equal to

$$\left\langle j_{\rm inj}^5\right\rangle'_p = \frac{15}{8}\left(\frac{\nu}{\mathcal{B}}\right)^{5/2}\alpha\left(\nu^2-\frac{1}{4}\right)\Gamma[\nu]\,{}_3\tilde{F}_2$$
$$\times\left[\frac{1}{2},\frac{7}{2},\nu;\frac{3}{2},\nu+\frac{9}{2};-\alpha^2\right], \tag{D27}$$

with

$$\langle j_{\rm inj}^5\rangle_p = \sum_{n=0}^{5}\binom{5}{n}\langle j_{\rm inj}^n\rangle_p' \omega^{5-n} \tag{D28}$$

and from the dynamics

$$\begin{aligned}\langle j_{\rm inj}^5\rangle = {} & \frac{15\alpha\gamma^3\hat{k}^5\mathcal{T}^5}{\Lambda\delta_\gamma^5[25k+\alpha(4\gamma+\hat{\gamma})](4km+3\gamma^2)[km+(\hat{\gamma}+\gamma)(\hat{\gamma}+2\gamma)+][9km+\hat{\gamma}(3\gamma+\hat{\gamma})]}\\ & \times\left[3\alpha^2\gamma^2\hat{\gamma}^2(\gamma+\hat{\gamma})^2(2\gamma+\hat{\gamma})(3\gamma+\hat{\gamma})+k^3m\left(12672\gamma^4+29768\gamma^3\delta_\gamma+27573\gamma^2\delta_\gamma^2+12058\gamma\delta_\gamma^3+2124\delta_\gamma^4\right)\right.\\ & +18k^4m^2\left(256\gamma^2+1025\gamma\delta_\gamma+450\delta_\gamma^2\right)+\alpha\hat{\gamma}(\gamma+\hat{\gamma})k\left(1008\gamma^5+2022\gamma^4\delta_\gamma+1209\gamma^3\delta_\gamma^2+305\gamma^2\delta_\gamma^3+42\gamma\delta_\gamma^4+4\delta_\gamma^5\right)\\ & \left.+k^2\left(6912\gamma^6+25464\gamma^5\delta_\gamma+34204\gamma^4\delta_\gamma^2+21733\gamma^3\delta_\gamma^3+7561\gamma^2\delta_\gamma^4+1598\gamma\delta_\gamma^5+172\delta_\gamma^6\right)\right].\end{aligned} \tag{D29}$$

APPENDIX E: COEFFICIENTS OF EQ. (25)

The coefficient of the term of first order in φ in the numerator is

$$A_1 = 2\sqrt{\frac{\mathcal{B}}{\pi\nu}}\frac{\Gamma[\nu]}{\Gamma\left[\nu-\frac{1}{2}\right]}\,{}_2F_1\left[\frac{1}{2},\nu;\frac{3}{2};-\frac{\mathcal{B}\varphi^2}{\nu}\left(\sqrt{\frac{\nu}{\mathcal{B}}}-2a\right)^2\right] \tag{E1}$$

and in the denominator equals

$$B_1 = 2\sqrt{\frac{\mathcal{B}}{\pi\nu}}\frac{\Gamma[\nu]}{\Gamma\left[\nu-\frac{1}{2}\right]}\,{}_2F_1\left[\frac{1}{2},\nu;\frac{3}{2};-\varphi^2\right]. \tag{E2}$$

With respect to the terms of third order in φ they would read

$$A_3 = \frac{4}{3}\sqrt{\frac{\mathcal{B}}{\pi\nu}}\frac{\Gamma[\nu]}{\Gamma\left[\nu-\frac{1}{2}\right]}(x-\omega)[2\omega\mathcal{B}(x+\omega)-\sqrt{\mathcal{B}\nu}(x+3\omega)+\nu]\,{}_2F_1\left[\frac{3}{2},\nu+1;\frac{5}{2};-\frac{\mathcal{B}\varphi^2}{\nu}\left(\sqrt{\frac{\nu}{\mathcal{B}}}-2\omega\right)^2\right] \tag{E3}$$

and

$$B_3 = \frac{4}{3}\sqrt{\frac{\mathcal{B}}{\pi\nu}}\frac{\Gamma[\nu]}{\Gamma\left[\nu-\frac{1}{2}\right]}(x+\omega)[\sqrt{\mathcal{B}\nu}(x-\omega)+\nu]\,{}_2F_1\left(\frac{3}{2},\nu+1;\frac{5}{2};-\varphi^2\right) \tag{E4}$$

for the numerator and the denominator, respectively.

[1] N. G. van Kampen, *Stochastic Processes in Physics and Chemistry* (Elsevier, Amsterdam, 2007).

[2] G. Gallavotti and E. G. D. Cohen, Phys. Rev. Lett **74**, 2694 (1995); J. Stat. Phys. **80**, 931 (1995).

[3] *Nonequilibrium Statistical Physics of Small Systems: Fluctuation Relations and Beyond*, edited by R. Klages, W. Just, and C. Jarzynski (Wiley-VCH, Weinheim, 2013); Y. Demirel, *Nonequilibrium Thermodynamics: Transport and Rate Processes in Physical and Biological Systems* (Elsevier, Amsterdam, 2014).

[4] T. S. Druzhinina, S. Hoeppener, and U. S. Schubert, Nano Lett. **10**, 4009 (2010).

[5] A. A. Balandin, Nat. Mater. **10**, 569 (2011).

[6] S. Schnell, T. J. H. Vlugt, J.-M. Simon, D. Bedeaux, and S. Kjelstrup, Chem. Phys. Lett. **504**, 199 (2011).

[7] K. Fujita, M. Iwaki, A. H. Iwane, L. Marcucci, and T. Yanagida, Nat. Commun. **3**, 956 (2012).

[8] A. Levy and R. Kosloff, Phys. Rev. Lett. **108**, 070604 (2012).

[9] M. Osiak, W. Khunsin, E. Armstrong, T. Kennedy, C. M. Sotomayor Torres, K. M. Ryan, and C. O'Dwyer, Nanotechnology **24**, 065401 (2013).

[10] K. Kanazawa, T. G. Sano, T. Sagawa, and H. Hayakawa, Phys. Rev. Lett. **114**, 090601 (2015); J. Stat. Phys. **160**, 1294 (2015).

[11] H. C. Andersen, J. Chem. Phys. **72**, 2384 (1980); P. H. Hünenberger, Adv. Polym. Sci. **173**, 105 (2005).

[12] W. T. Coeffly, D. A. Garanin, and D. J. McCarthy, Adv. Chem. Phys. **117**, 483 (2001).

[13] T. Czernik, J. Kula, J. Łuczka, and P. Hänggi, Phys. Rev. E **55**, 4057 (1997).

[14] A. Baule and E. G. D. Cohen, Phys. Rev. E **79**, 030103 (2009).

[15] R. Belousov, E. G. D. Cohen, and L. Rondoni, Phys. Rev. E **94**, 032127 (2016).

[16] M. J. I. Müller, S. Klumpp, and R. Lipowsky, Biophys. J. **98**, 2610 (2010); A. Kunwar, S. K. Tripathy, J. Xu, M. K. Mattson, P. Anand, R. Sigua, M. Vershinin, R. J. McKenney, C. C. Yu, A. Mogilner, and S. P. Gross, Proc. Natl. Acad. Sci. USA **108**, 18960 (2011).

[17] A. Gitterman, Physica A **221**, 330 (1995).

[18] A. B. Kolomeisky and M. E. Fisher, Annu. Rev. Phys. Chem. **58**, 675 (2007).

[19] W. A. M. Morgado and S. M. Duarte Queirós, Phys. Rev. E **86**, 041108 (2012).

[20] W. A. M. Morgado, S. M. Duarte Queirós, and D. O. Soares-Pinto, J. Stat. Mech. (2011) P06010; W. A. M. Morgado and S. M. Duarte Queirós, Phys. Rev. E **93**, 012121 (2016).
[21] G. H. Weiss, J. Stat. Phys. **15**, 157 (1976); F. Julicher, A. Ajdari, and J. Prost, Rev. Mod. Phys. **69**, 1269 (1997); C. R. Doering and J. C. Gadoua, Phys. Rev. Lett. **69**, 2318 (1992).
[22] G. Pfister and H. Scher, Adv. Phys. **27**, 747 (1978).
[23] J. Giddings and H. Eyring, J. Phys. Chem. **59**, 416 (1955).
[24] D. Taubert, M. Pioro-Ladrière, D. Schröer, D. Harbusch, A. S. Sachrajda, and S. Ludwig, Phys. Rev. Lett. **100**, 176805 (2008); N. Nishiguchi, *ibid.* **89**, 066802 (2002); Y. Jung, E. Barkai, and R. J. Silbey, Chem. Phys. **284**, 181 (2002); R. G. Neuhauser, K. T. Shimizu, W. K. Woo, S. A. Empedocles, and M. G. Bawendi, Phys. Rev. Lett. **85**, 3301 (2000).
[25] M. Anvari, G. Lohmann, M. Wächter, P. Milan, E. Lorenz, D. Heinemann, M. R. R. Tabar, and J. Peinke, New J. Phys. **18**, 063027 (2016).
[26] J. Łuczka, T. Czernik, and P. Hänggi, Phys. Rev. E **56**, 3968 (1997); I. Bena, C. Van den Broeck, R. Kawai, and K. Lindenberg, *ibid.* **66**, 045603(R) (2002).
[27] M. O. Cáceres and A. A. Budini, J. Phys. A **30**, 8427 (1997); M. O. Cáceres, Phys. Rev. E **67**, 016102 (2003); A. A. Budini and M. O. Cáceres, J. Phys. A **37**, 5959 (2004).
[28] P. Allegrini, P. Grigolini, and B. J. West, Phys. Rev. E **54**, 4760 (1996); P. Allegrini, P. Grigolini, L. Palatella, and B. J. West, *ibid.* **70**, 046118 (2004).
[29] L. Novotny, R. X. Bian, and X. S. Xie, Phys. Rev. Lett. **79**, 645 (1997).
[30] D. Applebaum, *Lévy Processes and Stochastic Calculus* (Cambridge University Press, Cambridge, 2004).
[31] H. Mori, Prog. Theor. Phys. **33**, 423 (1965); *1965 Tokyo Summer Lectures in Theoretical Physics*, edited by R. Kubo (Benjamin, New York, 1966).
[32] J. R. Medeiros and S. M. Duarte Queirós, Phys. Rev. E **92**, 062145 (2015).
[33] W. A. M. Morgado and S. M. Duarte Queirós, Phys. Rev. E **90**, 022110 (2014).
[34] H. Touchette and E. G. D. Cohen, Phys. Rev. E **76**, 020101(R) (2007).